The band model for the ground state properties of gadolinium metal

The band model for the ground state properties of gadolinium metal

W M Temmerman and P A Sterne†
SERC Daresbury Laboratory, Warrington WA4 4AD, UK

Abstract. We describe the electonic structure of Gd within the local spin density functional approximation treating the 4f electrons on equal footing with the s, p, d valence electrons. This band model is solved with the LMTO-ASA method, which includes the spin–orbit coupling and spin polarisation. The model gives a reasonable description of electronic structure properties such as the spin magnetic moment and the Fermi surface. Total energy calculations indicate that the experimentally observed HCP structure is favoured over both FCC and DHCP structures. Freezing the 5p semi-core states overestimates the lattice constant by 3.9%, while relaxing them as band states gives an underestimation of 3.4%, indicating a strong sensitivity to the treatment of these states.

1. Introduction

The local spin density functional approximation (LSD) provides an extremely successful and unified framework for describing the electronic properties of solids. In the rare earth metals, however, some doubt exists as to whether their properties can be described within the LSD. At issue is whether the electronic structure of such highly correlated f-electron systems can be based on a model where the exchange and correlation is derived from the exchange and correlation of a homogeneous electron gas. Furthermore, the subject is confused by the fact that the LSD should only be used to describe ground state properties, like lattice constants and magnetic moments, while the effects of the f-electron correlation are most apparent in excited state properties, such as photoemission and inverse photoemission spectra. Those controversies also arose, but to a lesser degree, in the electronic structure of transition metals. However, for the transition metals the argument was settled by the numerous band calculations which gave excellent agreement with a variety of experiments. Unfortunately progress in the electronic structure of rare earth metals has been hampered by technical difficulties in performing accurate self-consistent field calculations, making the exact status of the LSD with respect to the rare earth metals not as clear cut. The first self-consistent field (SCF) calculation for Gd was performed by Harmon (1979). Since then only three other calculations have been performed: Sticht and Kubler (1985), Krutzen and Springelkamp (1989) and the present work (1989).

† Present address: Division of Chemistry and Materials Science (L-280), Lawrence Livermore National Laboratory, University of California, Livermore, California 94550, USA.

It is argued by Skriver (1982) that in the presence of localised states band theory will give too small a lattice constant, i.e. it will overestimate the bonding. Our study therefore focuses on the contribution of the 4f and also 5p bonding in the determination of the lattice constant of Gd. We will also discuss how accurately the band model is solved. This is crucial to know in relation to the various schemes to improve on the LSD, such as the self-interaction correction (SIC) (Perdew and Zunger 1981) and the gradient corrections (Langreth and Mehl 1983).

In this paper we will compare our LSD calculations for Gd with both the ground state properties and the electronic energy bands as derived from the de Haas–van Alphen measurements (Mattocks and Young 1977, Young 1979). Traditionally, the electronic structure of rare earth metals has been described by two contrasting methods depending on which properties one is interested in (Gschneider and Eyring 1978). A band model with s, p, d electrons and the f electrons frozen in the core is used to describe the de Haas–Van Alphen measurements, the transport properties, the crystal structures etc, while a crystal field model, where the f electrons play a central role but that completely neglects the valence s, p, d electrons, describes the magnetic properties. However neither model on its own can explain all the electronic properties. The purpose of our paper is to investigate whether the LSD is capable of doing this. We therefore discuss the Fermi surface and the lattice constant and investigate the f contributions to it. We also calculate the spin magnetic moment and study the contributions due to the conduction electron polarisation.

The organisation of this paper is as follows. The next section discusses the band model and our technique for solving this model. In section 3 we give the energy bands, the density of states and the Fermi surface. Section 4 analyses the bonding properties and section 5 studies the role of the 5p semi-core states in the bonding. Section 6 discusses and summarises our findings.

2. The band model and the electronic structure method

We use the linear muffin tin orbital (LMTO) method in the atomic sphere approximation (ASA) (Andersen 1975, 1984, Skriver 1984) to solve the LSD equations (von Barth and Hedin 1972). This method has been used with great success to describe the electronic structure of elemental solids and complicated systems (Andersen *et al* 1985). It is a fast band structure method at the expense of only a small loss in accuracy. The ASA replaces the Wigner–Seitz polyhedra of the solid by overlapping Wigner–Seitz spheres. This approximation is most accurate for close-packed elemental metals. The band structure method is a basis set method with only one basis function per angular momentum. To treat the electronic structure in the energy range of both the semi-core 5p and the conduction 6p orbitals we use two energy panels with a different set of basis functions for each panel.

An electronic structure study of Gd has to take into account the relativistic effects in the presence of spin polarisation. Band theorists have recently become interested in the interplay of relativistic effects with spin ordering. All total energy calculations up to now have been performed using a perturbational approach which includes the $L \cdot S$ coupling in the Hamiltonian but not in the basis functions (Brooks and Kelly 1983, Sticht and Kubler 1985). However, band theory has been generalised to treat spin polarisation and all relativistic effects on equal footing by Feder *et al* (1983) and Strange *et al* (1984) in the case of KKR band method; by Ebert (1988) for the LMTO–ASA method; by Krutzen
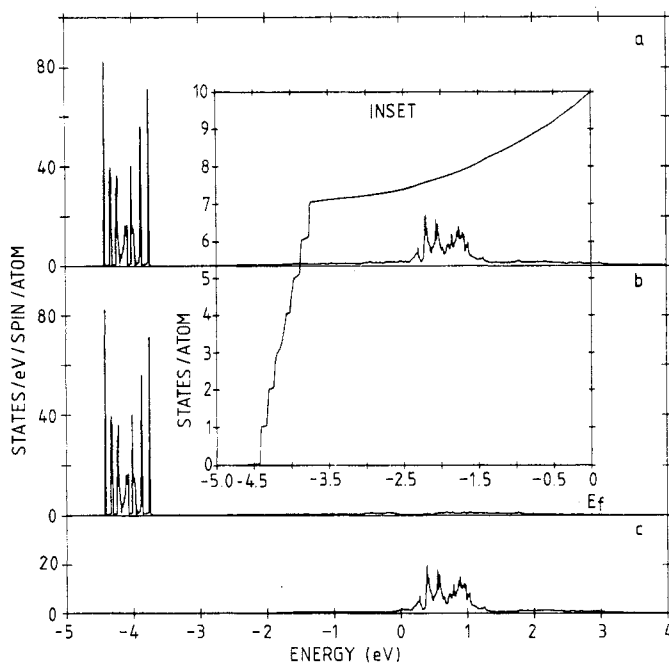
Figure 1. The total density of states of Gd (*a*), decomposed into the majority spin contribution (*b*), and the minority spin contribution (*c*). The inset is the integrated density of states of the occupied bands. In this calculation the 5p states were kept in the frozen core and spin–orbit coupling was included (HCP-PF-SO case of table 1).

and Springelkamp (1989) for the ASW and by Richter and Eschring (1989) for the LCAO formalism. Our calculations use the variational approach (Sticht and Kubler 1985) with the LMTO-ASA band structure scheme. We argue from the results of our calculation that the spin–orbit splitting in Gd is much smaller than the spin splitting, validating *a posteriori* our approach.

We performed LMTO-ASA calculations for a spin-polarised scalar–relativistic Hamiltonian with the spin–orbit coupling included variationally using the Koelling and Harmon (1977) form. We used the von Barth–Hedin form for the local exchange and correlation and treated the 4f electrons of Gd as valence states. During the calculations we iterate the 4f, 6s, 6p and 5d contributions to the charge density to self-consistency. All the other orbitals, obtained from a relativistic atomic calculation, are kept frozen during this iteration process. The Brillouin zone integrations were carried out using the tetrahedron method. In contrast to earlier LMTO calculations (Skriver 1982) these integrals were carried out analytically, avoiding the need for a numerical integration over a fine energy mesh. We also calculated the charge density directly, from the wave function coefficients, rather than using the more common and less accurate moment expansion (Skriver 1982). These technical improvements (Temmerman *et al* 1989) led to a dramatic improvement in the rate and stability of convergence, so stability in the converged total energy of better than 1 μRyd is readily obtainable.

We use a value of 3.764 au for the experimental Wigner–Seitz radius (Skriver 1984) and in all the calculations we use the experimental *c/a* ratio, which is 2.57% smaller than the ideal HCP *c/a* ratio. The Brillouin zone integrals were performed with the linear
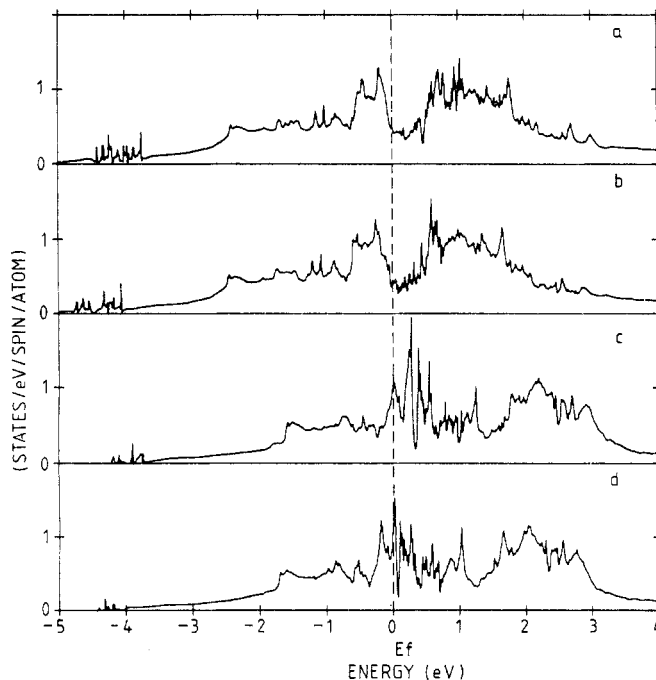
Figure 2. The influence of relaxing the 5p semi-core states on the s + p + d density states; (*a*), (*b*) majority spin contributions for respectively the 5p frozen in the semi-core (HCP-PF-SO case of table 1) and the 5p treated as band states (HCP-PR-SO case of table 1); (*c*), (*d*) minority spin contributions for respectively HCP-PF-SO and HCP-PR-SO.

tetrahedron method using 112 *k*-points in the irreducible HCP Brillouin zone. Finally, all the calculations were performed without combined correction term.

3. Electronic structure of Gd

In the first four figures we present our results for the density of states, energy bands and Fermi surface of Gd at the experimental lattice constant. The calculations include the spin–orbit splitting and are for a frozen core which include the 5p core levels. In figure 1 the total density of states is projected onto the spin up and spin down states. The density of states is dominated by the majority and minority f states. The LSD calculation clearly indicates that the atomic-like f electrons obey Hund's rules, occupying the first seven states with parallel spin. The majority ones, from 3.7 eV to 4.4 eV below E_F, are split up in seven narrow sub-peaks, through the combined effect of the crystal field, spin–orbit and exchange splitting. The minority f states are broader, extending from just above the Fermi energy to more than 1 eV above it. The integrated density of states (inset to figure 1) increases in steps of one electron when the energy moves through the majority f states. In figure 2 we show the s + p + d contribution to the density of states decomposed according to spin. The occupied majority and minority states are more or less rigidly shifted by 0.8 eV with respect to each other, giving rise to a 'conduction' electron contribution of 0.678 μ_B to the total magnetic moment of 7.548 μ_B. The density of states at E_F is dominated by the s + p + d electrons: $n(E_F) = 25.326$ states Ryd^{-1}/
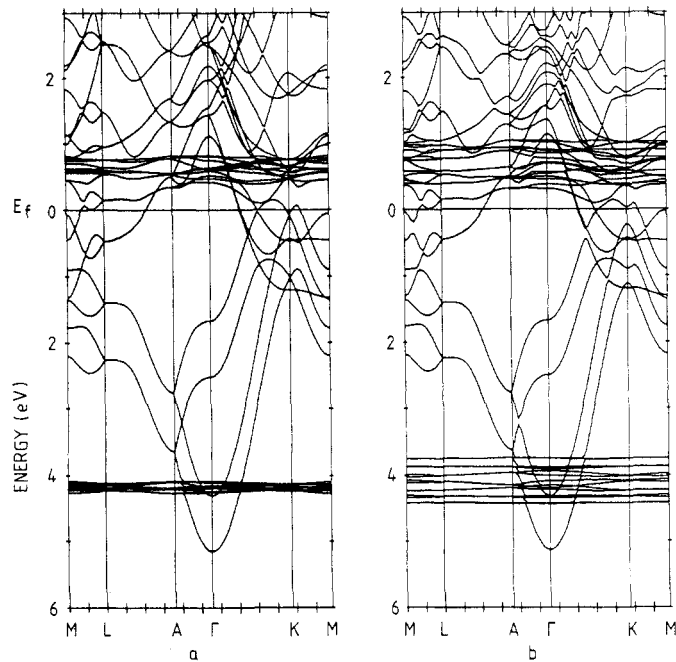
Figure 3. The effects of the spin–orbit coupling on the band structure in some high symmetry directions of the HCP Brillouin zone: (*a*) no spin–orbit coupling (case HCP-PF of table 1), (*b*) with spin–orbit coupling (case HCP-PF-SO of table 1).

atom of which the f contribution is small (5.815 states Ryd^{-1}/atom). Neglecting the spin–orbit coupling (figure 3) reduces the majority f band width from 0.7 eV to 0.2 eV, without, however, affecting the centroid position of the f levels.

The difference between the number of electrons in the majority and minority bands determines the spin contributions to the magnetic moment. We obtain a value of 7.548 μ_B, in excellent agreement with the experimental value of 7.63 μ_B (Roeland *et al* 1975). Krutzen and Springelkamp obtain 7.55 μ_B, identical to our moment for the same exchange and correlation potential. However, the conduction electron contribution (spd electrons only) to our moment is 0.678 μ_B, which is slightly smaller than Krutzen and Springelkamp's value of 0.736 μ_B. The density of states at E_F of our calculation is low: 25.326 states Ryd^{-1}/atom in good agreement with the values deduced from the low temperature specific heat (21.35) (Wells *et al* 1974) and substantially smaller than the value of 46.74 from Sticht and Kubler and 36.72 from Krutzen and Springelkamp. Our value is small because we have the unoccupied f electrons well separated from E_F: 0.3 eV above E_F in comparison with 0.1 eV in the calculations of Sticht and Kubler and Krutzen and Springelkamp.

There are three basic Fermi surface sheets in Gd: two majority, hole carriers, surfaces and a minority, electron carrier, surface (Mattocks and Young 1977). We identify bands 20 and 21 in figure 4 as the hole surfaces, predominantly of majority character, and band 22 as the electrons surface, mostly of minority character. We superimpose on our Fermi surface the Fermi surface deduced by Mattocks and Young from de Haas–Van Alphen measurements. We note the very good agreement of the 'majority surfaces' between Mattocks and Young's model and our calculation. Concerning the minority surface there
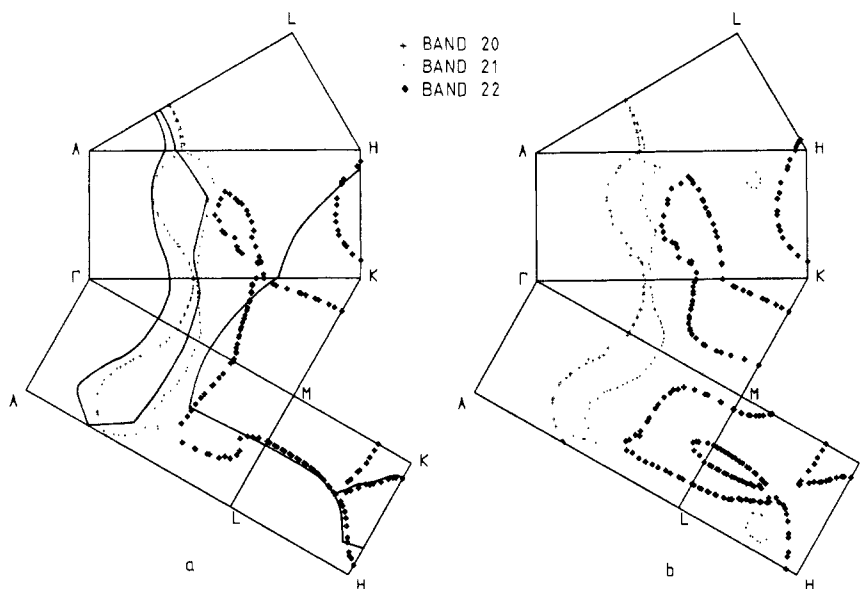
Figure 4. The calculated and experimental (full line) Fermi Surface (Mattocks and Young) of Gd; (*a*) refers to the case HCP-PF-SO, (*b*) to HCP-PR-SO. The various sheets are identified by the band indices 20, 21 and 22.

are some topological differences, but we agree with Mattocks and Young's value of the exchange splitting of 0.8 eV between minority and majority bands. However, Mattocks and Young find several low frequencies which could not be identified on the above three surfaces, indicating that the minority Fermi surface may be more complicated. Our results show that such small pieces of Fermi surface are present, for example around the K point. This minority surface is very sensitive to the position of the unoccupied f levels as will be discussed in section 5.

4. Bonding and crystal structure

We obtain a theoretical lattice constant that is 3.9% too big (figure 5). This is very different from the result of Sticht and Kubler, who obtain a lattice constant that is 2.5% too small. Our theoretical bulk modulus is 47.4 GPa, an overestimation of the experimental value of 41 GPa and 39 GPa as obtained by Sticht and Kubler. The reason for the difference of more than 6% between Sticht and Kubler's calculation and ours is related to the position of the minority f with respect to E_F. In Sticht and Kubler's calculation the minority f are closer to E_F: 0.1 eV above E_F; in ours, 0.3 eV. This will give rise to more f bonding, resulting in a smaller lattice constant.

Neglecting the spin–orbit coupling does not change the theoretical lattice constant as can be seen from figure 5. On the basis of this result, we studied the theoretical crystal structure by performing self-consistent calculations without the spin–orbit splitting. We calculated the total energies of FCC Gd (as three interpenetrating HCP structures) and DHCP Gd (four atoms per unit cell) using the same density of k-points in the irreducible

Table 1. The total energy (Ryd/atom) (E_T) at the experimental lattice constant, the band contribution (E_B), the Coulomb (E_C) and the exchange and correlation contribution (E_{XC}) for the HCP, DHCP, FCC structures with either the 5p levels frozen (PF) or 5p relaxed as band states (PR) and with the spin–orbit included (SO) in the first and last columns only. A decomposition according to angular momentum and spin of the total number of valence electrons per atom (N) is given. The total spin magnetic moment is decomposed into the f and s + p + d contributions. The total density of states per atom and rydberg and its f contribution are given in the last two lines.

	HCP-PF-SO	HCP-PF	DHCP-PF	FCC-PF	HCP-PR-SO
E_T	−75.5988	−75.5876	−75.5872	−75.5854	−76.3609
E_B	−3.9480	−3.9856	−3.9356	−3.9146	−4.1227
E_{XC}	−28.1990	−28.2040	−28.2044	−28.2069	−28.3539
E_C	−43.4518	−43.3980	−43.4472	−43.4639	−43.8843
$N_s^\uparrow$	0.399	0.399	0.396	0.394	0.397
$N_s^\downarrow$	0.382	0.382	0.387	0.386	0.380
N_s^{tot}	0.781	0.781	0.783	0.780	0.777
$N_p^\uparrow$	0.340	0.344	0.308	0.305	0.320
$N_p^\downarrow$	0.166	0.163	0.174	0.166	0.165
N_p^{tot}	0.506	0.507	0.482	0.471	0.485
$N_d^\uparrow$	1.048	1.067	0.998	1.007	1.011
$N_d^\downarrow$	0.560	0.552	0.632	0.636	0.571
N_d^{tot}	1.608	1.619	1.630	1.643	1.582
$N_f^\uparrow$	6.987	7.015	7.011	7.011	6.986
$N_f^\downarrow$	0.117	0.078	0.093	0.096	0.170
N_f^{tot}	7.104	7.093	7.104	7.107	7.156
μ_B^{tot}	7.548	7.650	7.428	7.433	7.426
μ_B^f	6.870	6.937	6.918	6.915	6.816
μ_B^{s+p+d}	0.678	0.713	0.510	0.518	0.610
$n(E_F)$	25.326	22.233	26.069	28.900	35.124
$n_f(E_F)$	5.814	4.566	6.152	4.759	12.000

Brillouin zone wedge. Our results are summarised in table 1 and figure 5. We obtain the HCP structure as the theoretical ground state structure in comparison with the DHCP and FCC structures. The energy is lowered by respectively 0.92 and 3.06 mRyd. The lattice constant in these three structures is approximately 4% too big. From the total energy (E_T) decomposition, at the experimental lattice constant, into the band structure (E_B), an electrostatic term (E_C) and exchange and correlation (E_{XC}):

$$E_T = E_B + E_C + E_{XC}$$

we see that the band structure term is 50 mRyd lower in the HCP structure than in the DHCP one, and 71 mRyd lower than in the FCC one. The electrostatic terms on the other hand favour FCC over DHCP over HCP. We obtain 1.6 d electrons in all the structures and this is consistent with the HCP crystal structure according to Duthie and Pettifor (1977).

5. The 5p semi-core states

The 5p levels do not really behave as true core states. Even though their binding energy is more than 10 eV below the bottom of the valence bands, the 5p shell is spatially outside
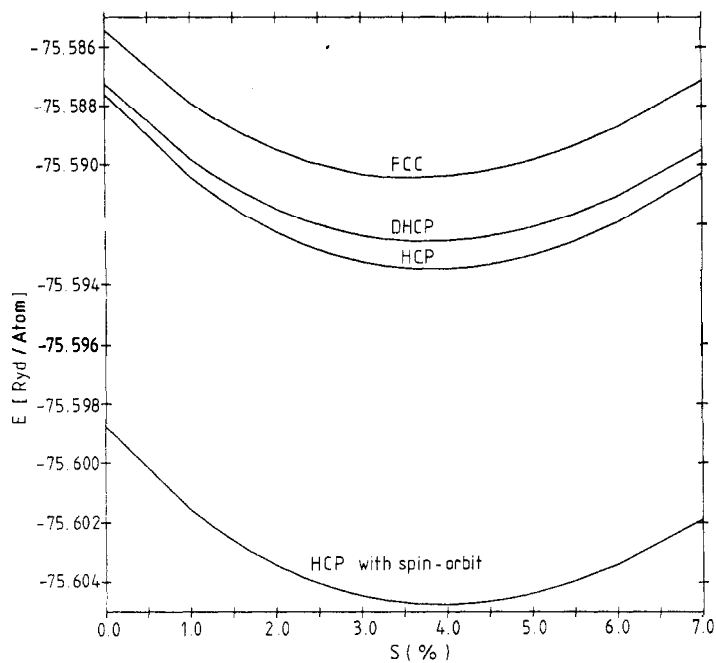
Figure 5. The total energies as a function of deviation of the experimental Wigner–Seitz radius for Gd in the FCC, DHCP, HCP and HCP with spin–orbit included. The decomposition of these total energies at the experimental Wigner–Seitz radius is given in table 1 in the columns FCC–PF, DHCP–PF, HCP–PF and HCP–PF–SO respectively.
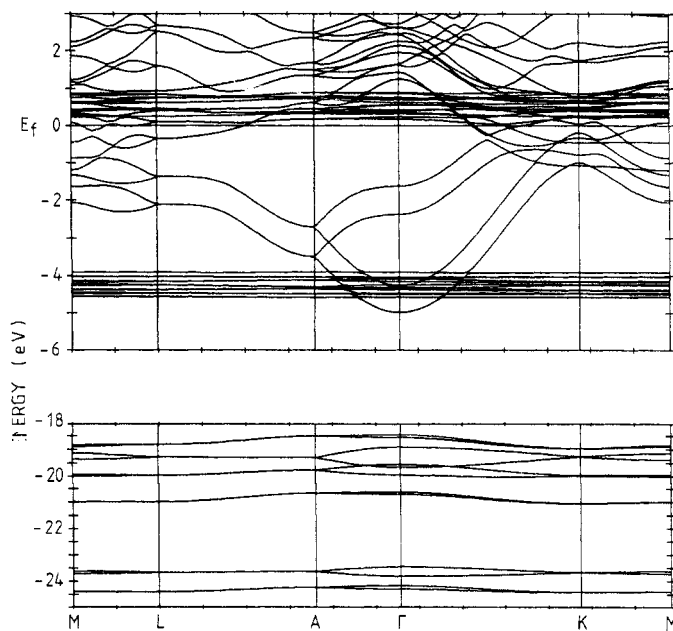

Figure 6. The semi-core and valence band structure of Gd corresponding to the column HCP–PR–SO of table 1.

the 4f shell. We therefore performed self-consistent field calculations with the 5p states treated as band states through the use of panels. Our resulting band structure is shown in figure 6. This shows that the 5p states do indeed have some dispersion. The unoccupied f states are lowered by 0.1 eV, the occupied ones by 0.2 eV. The density of states at the Fermi energy increases from 25.326 states Ryd^{-1}/atom to 35.124, with the f contribution increasing from 5.814 to 12.0 (table 1). The f contribution to the spin moment is reduced from 6.870 to 6.816, which reduces the conduction electron contribution from 0.678 to 0.610.

The effect of lowering of the f bands on the conduction bands on the conduction bands is studied in figures 2(*b*) and 4(*b*). The exchange splitting is reduced from 0.8 eV to 0.7 eV. The Fermi energy went up (figure 2(*b*)), so the hole Fermi surfaces (figure 4(*b*)) have increased. Bringing the minority f levels closer to E_F has changed the topology of the Fermi surface due to band 22. For example band 22 does not cross the ΓM direction any more. Unfortunately, current fermiology results (Mattocks and Young 1977, Hoffmann *et al* 1982, Waspe and West 1982) do not distinguish between 4(*a*) and 4(*b*).

But, most dramatically, including the 5p as band states out of the frozen core has reduced the lattice constant from +3.9% to −3.4%, by more than 7%!!

6. Discussion and conclusion

The position of the minority f levels crucially affects the lattice constant. Relaxing the semi-core 5p states changes the lattice constant by 7% by lowering the 4f levels by as little as 0.1 eV. The reduction of the lattice constant by 7% is not solely due to the lowering of the minority f levels. In the case of Y relaxing the 5p semi core levels reduces the lattice constant by 2% (table 2). As can be seen from this table there are substantial reductions in lattice constant on relaxing the p semi-core states of the early transition metals. On the other hand KKR calculations for Y (Guo *et al* 1989, 1990) find that the lattice constant increases by 3% from −6% to −3% on relaxing the p semi-core states; this lattice constant of −3% compares well with a lattice constant of −2.6% from the LMTO–ASA.

The big discrepancy between Sticht and Kubler's lattice constant of −2.5% and ours of 3.9% becomes a reasonable agreement when we compare our lattice constant with relaxed 5p states of −3.4% with Sticht and Kubler's result of −2.5%. Moreover, we found that it was not important to treat the 5p states as band states, as an all electron calculation with the 5p relaxed as core states gave us a similar lattice constant of −3.4%.

Table 2. The theoretical lattice constants for some of the early transition metals in the 3d, 4d and 5d rows with the p semi-core either frozen or relaxed as band states.

Ca	Sc	Ti	V	
−3.51	−1.77	−1.37	−1.6	3p frozen
−4.67	−2.90	−2.64	−2.96	
	Y	Zr	Nb	
	−0.87	−0.19	0.2	4p frozen
	−2.64	−1.61	−1.44	
	La	Hf	Ta	
	+3.3	−0.19	0.0	5p frozen
	−2.34	−0.60	−0.99	

Finally we note that Sticht and Kubler's result also refers to an all electron calculation. From all this we can conclude that the 5p semi-core states play a crucial role in determining the lattice constant of Gd—the LSD resulting in over-estimating the 5p bonding. More work is now needed to establish what improvements to LSD, such as SIC, are needed to localise the 5p states sufficiently to obtain a better agreement in theoretical lattice constants.

We conclude that for the soft rare earth metals with their very localised states, the evaluation of the theoretical lattice constant is an extremely sensitive test of the LSD. But surprisingly we have to turn our attention to an improved LSD treatment of the 5p states in Gd. An experimental determination of the Fermi surface of band 22 would give us a quantity that would be another crucial test for a calculation. Finally we can summarise by saying that LSD can be used to provide this unified description of both localised and band-like features in elemental Gd.

References

Andersen O K 1975 *Phys. Rev.* B **12** 3060
—— 1984 *The Electronic Structure of Complex Systems (NATO ASI Series B, vol 113)* ed P Phariseau and W M Temmerman (New York: Plenum) p 11
Andersen O K, Jepson O and Glotzel D 1985 *Highlights of Condensed Matter Theory* ed F Bassani, F Fumi and M P Tosi (Amsterdam: North-Holland)
Brooks M S S and Kelly P J 1983 *Phys. Rev. Lett.* **51** 1708
Duthie J C and Pettifor D G 1977 *Phys. Rev. Lett.* **38** 564
Ebert H 1988 *Phys. Rev.* B **38** 9391
Feder R, Rosicky F and Ackermann 1983 *Z. Phys.* B **52** 31
Gschneider K A Jr and Eyring L (ed) 1978 *Handbook on the Physics and Chemistry of Rare Earths* (Amsterdam: North-Holland)
Guo G Y, Temmerman W M and Szotek Z 1989 Ψ_k *Newsletter* **13** 14
—— 1990 to be submitted
Harmon B N 1979 *J. Physique Coll.* **40** C5 65
Hoffmann K R, Berko S and Beaudry B J 1982 *Positron Annihilation* ed. P G Coleman, S C Sharma and L M Diana (Amsterdam: North-Holland) p 325
Koelling D D and Harmon B N 1977 *J. Phys. C: Solid State Phys.* **10** 3107
Krutzen B C H and Springelkamp F 1989 *J. Phys.: Condens. Matter* **1** 8369
Langreth D C and Mehl M J 1983 *Phys. Rev.* B **28** 1809
Mattocks P G and Young R C 1977 *J. Phys. F: Met. Phys.* **7** 1219
Perdew J P and Zunger A 1981 *Phys. Rev.* B **10** 5048
Richter M and Eschrig H 1989 *Solid State Commun.* **72** 263
Roeland L W, Cock G J, Muller F A, Moleman A C, McEwan K A M, Jordan R C and Jones D W 1975 *J. Phys. F: Met. Phys.* **5** L233
Skriver H L 1982 *Systematics and the Properties of the Lanthanides* ed S P Sinha (Dordrecht: Reidel)
—— 1984 *The LMTO Method* (Berlin: Springer)
Sticht J and Kubler J 1985 *Solid State Commun.* **53** 529
Strange P, Staunton J B and Gyorffy B L 1984 *J. Phys. C: Solid State Phys.* **17** 3355
Temmerman W M, Sterne P A, Guo G Y and Szotek Z 1990 *Mol. Simul.* **4** 153
von Barth U and Hedin L 1972 *J. Phys. C: Solid State Phys.* **5** 1629
Waspe R L and West R N 1982 *Positron Annihilation* ed P G Coleman, S C Sharma and L M Diana (Amsterdam: North-Holland) p 328
Wells P, Lanchester P C, Jones D W and Jordan R G 1974 *J. Phys. F: Met. Phys.* **4** 1729
Young R C 1979 *J. Physique Coll.* **40** C5 71